

DETC2009-86923

## GAIT AND GAIT TRANSITION FOR A ROBOT WITH TWO ACTUATED SPOKE WHEELS

### Ya Wang

RoMeLa: Robotics & Mechanisms Laboratory  
Mechanical Engineering Department  
Virginia Polytechnic Institute and State University  
Blacksburg, Virginia 24061  
Email: ywang07@vt.edu

### Ping Ren

RoMeLa: Robotics & Mechanisms Laboratory  
Mechanical Engineering Department  
Virginia Polytechnic Institute and State University  
Blacksburg, Virginia 24061  
Email: renping@vt.edu

### Dennis Hong<sup>1</sup>

RoMeLa: Robotics & Mechanisms Laboratory  
Mechanical Engineering Department  
Virginia Polytechnic Institute and State University  
Blacksburg, Virginia 24061  
Email: dhong@vt.edu

### ABSTRACT

This paper presents work on the gait and gait transition analysis for a novel mobile robot that uses two actuated spoke wheels. Gait transitions, known as acyclic feed forward patterns, allow the robot to switch from one type of gait to another during walking and turning. The mobile robot *IMPASS* (Intelligent Mobility Platform with Active Spoke System) uses a unique mobility concept for locomotion, thus gait transition plays an important role in generating gait patterns to walk and turn. The primary focus of this paper is how to perform gait transition between gaits in walking direction. First, the basic gait patterns for steering and straight line walking are presented. More specifically, the critical gait parameterizations and the possible foot positions in different gait patterns to produce capable steering locomotion over terrain are presented. Since *IMPASS* is expected to utilize its metamorphic configurations to carry out gait transitions, the extending forward and inverse analyses are also presented based on previous work about topology classification and mobility analysis for *IMPASS*. Then the gait transition analysis and simulation of typical patterns are performed. The results from this work lay the foundation for the future research on trajectory and path planning for *IMPASS*.

## 1 INTRODUCTION

RoMeLa (Robotics and Mechanisms Laboratory) at Virginia Tech proposed and designed a novel high-mobility locomotion platform, *IMPASS* (Intelligent Mobility Platform with Active Spoke System), as shown in Fig. 1, classified as the leg-wheel hybrid robots [1-4], which is much more adaptable to a wide range of unstructured ground environments than the wheeled

robots and faster on smooth surfaces than the legged robots. Previous work has been presented [5-6] on mobility and geometrical analysis, and the three-dimensional kinematic analysis of *IMPASS*.



Figure 1. One of the *IMPASS* Prototypes.

*IMPASS* is designed to walk on various terrains, cross over obstacles or climb up steps, using the unique ability to actuate its spokes intelligently. One approach to generate a walking motion, which is a context-dependent locomotive behavior, is to take abstracted view of feet locomotion by selecting the gaits a robot may use. The basic gait patterns will be stored with each gait designed for a specific purpose. In the absence of sensor information, intuitive feed forward motion patterns can be developed according to various tasks [7]. Learning techniques have been applied in this area to improve robustness and performance [8-9]. A hierarchical approach to robot control can then be taken, allowing the robot to walk by switching through a sequence of gaits. The control system can focus on selecting appropriate gaits and adjusting parameters of those gaits for general steering.

1. Address all correspondence to this author.

Gait and gait transition is a major component of the path planning, where many research works have been concentrated. For instance, McGhee and Iswandhi introduced a free gait, a non-periodic gait, in which any leg can move at any time to provide support and body motion on rough terrain [10]. Song and Waldron [11] proposed an analytical approach, where the foot position is defined by local phase, which is the fraction of a cycle period by which the current foot position follows the placement of that foot. This analytical approach promoted a better understanding of the leg coordination of a periodic gait. Hamdan, Fontaine, and Picard [12] presented a theoretical strategy of gait transitions for quadruped. They developed a graphical representation of gaits that allows the comparison and explanation of gait transition process. Zhang and Song [13] performed the study of quadruped turning gaits. Spinning gaits and circling gaits are introduced based on the location of the turning center. Tsujita, Kobayashi, Inoura and Masuda developed an oscillator method for gait transition controlling [14].

However, not that much research work mentioned above can be adapted for the application of IMPASS analysis due to the unique metamorphic configurations during its walking locomotion. Most likely, in this paper, we just borrowed the concepts and terminology from the previous research work. Instead of talking about the phase portrait of walking speed during the gait transition, we mainly focus on the metamorphic configuration of the gait and gait transition.

The remainder of the paper is organized as follows: with the database of possible gait patterns, the challenging task becomes how to specify the particular gait pattern and how to transit between them, in order to adapt to environmental changes in locomotion context, as the requirements to the underlying path planning are altered, which is described in section 2. The problem remaining is how to perform gait transition between gaits in walking direction, the primary focus of this paper, which is presented in section 3. More specifically, we address the critical gait parameterizations and the possible feet positions in different gait patterns to produce capable steering locomotion over terrain. In order to describe an automated behavioral sequence to enable the smooth transition, for example, even terrain steering, the strategies for transitioning between gait patterns are explored in section 3. In section 4, several typical gait pattern transition experimental tests are discussed to illuminate issues of the applications of open loop strategies on gait transitions. At the end, in section 5, conclusions are drawn and the future work is stated.

## 2 BASIC GAIT PATTERNS

In this paper, “gait” states a continuous motion that produces locomotion through a time starting with the foot departure from the ground to approach to the ground. In some paper [15], the term “stance” is used to denote the spoke that is in contact with the ground, while ‘flight’ refers to the spoke that is swinging through the air. During stance, the spoke pushes against the grounds, generating forces that move the robot

forward. A spoke in flight returns to the configuration where stance begins again, completing a cycle of the gait. Here, we will use the term “gait pattern” to denote the specific “ground contact case” we defined in reference [5], which enumerate all types of contact schemes *IMPASS* could have with the ground. As we know, *IMPASS* is designed with two actuated spoke wheels, connected through the axle, as shown in Fig.1. Each of the wheels is composed of three independently actuated spokes, which pass through the hub centers. In our previous paper, the kinematics models with variable configurations of *IMPASS* are classified into totally twenty ( $4+10+6=20$ ) ground contact cases [5] based on various ground contact points in left and right wheels. Considering the mobility, stability and efficiency of the walking locomotion, the following six gait patterns (ground contact cases) and their transitions of *IMPASS* are going to be adopted very often for the motion planning, as illustrated in Fig.2. Here, the positive direction of Y axis represents the forward direction of *IMPASS*. Note that, we still use the terminology  $n_1-n_2$  ( $n_1, n_2=0, 1, 2, \text{ or } 3$ ), [5] to represent ground contact case, that is, gait pattern. With respect to this forward direction,  $n_1$  denotes the number of actual contact points in the right spoke wheel while  $n_2$  stands for the number of actual contact points in the left spoke wheel.

In Fig.2, 1-1P pattern is corresponding to 1-1Parallel unequal case, that is, there is 1 right ground contact spoke, 1 left ground contact spoke, where both ground contact spokes are parallel with unequal effective spoke length( as defined in [5], effective spoke length represents the spoke length from the corresponding hub center to the ground). However, 1-1 P (E) denotes the 1-1 Parallel pattern with equal effective length. 2-1 pattern represents that there are 2 right and 1 left ground contact spokes. 1-1S indicates that each side has 1 ground contact spokes, but both ground contact spokes are in skew. Whereas 1-1S(R) pattern performs the right turn, 1-1S (L) pattern carries out the left turn. In the end, 2-2 pattern represents 2-2 parallel case with equal effective spoke length, when super stable structure is required.

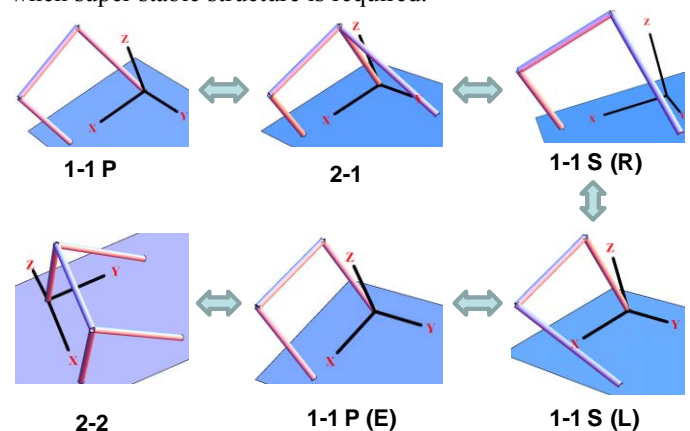


**Figure 2.** Gait Pattern Transitions during *IMPASS* Walking.

The common sense for path planning is the trajectory composed of circle line and straight line, that is, the combination of 1-1P pattern and 1-1P (E) pattern. However,

the gait transitions from 1-1P to 1-1P (E) include transition from 1-1P to 2-1 to 1-1S and then to 1-1P (E) pattern, where 1-1S could be 1-1S(R) or 1-1S (L). Well, the gait transition from 1-1S(R) pattern to 1-1(L) pattern is involved here, because this gait transition can perform the right to left or left to right sharp turning, whereas the others only execute right turn or left turn. In order to lay the foundation for the future trajectory planning, the following of this paper will focus on 1-1P gait and 1-1P to 1-1P (E) gait transition.

### 3 GAIT AND GAIT TRANSITIONS

With a large set of possible gait patterns, the challenging task becomes understanding how to perform transition between them in order to produce different styles of gaits. Different from gait, a periodic motion, gait transition is inherently acyclic, beginning at one robot configuration found in one gait pattern and ending at the configuration from another gait pattern. Whereas gaits are meant to be walk cyclically, transitions are acyclic behaviors that switch between gaits. We need to mention that “cyclic” and “acyclic” are used to describe the metamorphic configurations of gait and gait transition. In the study of path planning for an undergoing change of walking direction of *IMPASS*, for example, from circular line to straight line, 1-1P gait and 1-1P to 1-1P (E) gait transition are engaged (in Fig.2), which is the main focus of this section.

In order to generate useful transitions, it is important to understand the fundamental properties of gaits, such as their parameterizations, as well as issues like gait constraints and gait validity. A valid gait transition would be one that continues locomotion, changing a gait’s parameters from one gait to another over a finite period of time, while keeping the robot in valid configurations throughout the transition.

#### 3.1 1-1 P and 1-1P (E) Gait:

1-1P gait pattern plays very important roles when performing a circular locomotion with changeable curvature radius, whereas 1-1P (E) pattern is the vital pattern for straight line walking motion of *IMPASS*. To be convenience, we put these two patterns together, since they have the similar parameterizations for the walking motion. Without losing generality, we use 1-1P pattern represents both of them in this section. Note that, the curvature of a circle of radius "r" is its reciprocal "1/r" and the curvature is smaller the larger the radius of the circle.

The nomenclature definition for 1-1P gait pattern is shown in Table 1, and their geometrical meaning is also illustrated in Fig.3, Fig. 5 and Fig.6. These figures indicate the stance when both gait 1 and gait 2 contact the ground at the same time.

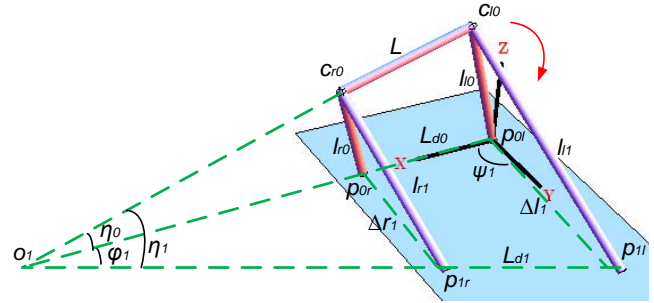


Figure 3. 1-1 P Pattern Stance from Gait 1 to Gait 2.

In the derivation, we choose a reference coordination system at each gait which superposes the left foot fixed coordinate system (attached to the left foot of *IMPASS*) at each gait. As shown in Fig. 3, the fixed global coordinate system XYZ is coincident with the reference coordinate system at Gait 1.

Table 1. Nomenclature for 1-1P Gait Pattern.

Symbol	Definition
$G(x, y, z)$	Global Cartesian Coordinate
$L$	Length of the axle
$l$	Full length of each spoke
$k$	Right /left effective spoke length ratio
$r_i$	Inner circle radius
$r_m$	Medial circle radius
$r_o$	Outer circle radius
$o_1 \dots o_i \dots o_n$	Turning center at Gait $i$ *
$l_{i0}, l_{i1} \dots l_{in} \dots l_{ln}$	Effective right spoke length at Gait $i+1$
$l_{r0}, l_{r1} \dots l_{ri} \dots l_{rn}$	Effective right spoke length at Gait $i+1$
$d_0, d_1 \dots d_i \dots d_n$	Medial spoke length at Gait $i+1$
$L_{d0} \dots L_{di} \dots L_{dn}$	Feet distance between the pair of parallel spokes at Gait $i+1$
$\Delta l_0 \dots \Delta l_i \dots \Delta l_n$	Effective spoke length difference between the pair of parallel spokes at Gait $i+1$
$\Delta l_1 \dots \Delta l_i \dots \Delta l_n$	Left step length during Gait $i$
$\Delta r_1 \dots \Delta r_i \dots \Delta r_n$	Right step length during Gait $i$
$\theta_0, \theta_1 \dots \theta_i \dots \theta_n$	Rotating angle at Gait $i+1$
$\psi_1, \psi_2 \dots \psi_i \dots \psi_n$	Heading angle at Gait $i$
$\eta_0, \eta_1 \dots \eta_i \dots \eta_n$	Rolling angle at Gait $i+1$
$\phi_1, \phi_2 \dots \phi_i \dots \phi_n$	Turning angle at Gait $i$
$c_{i0}, c_{i1} \dots c_{in} \dots c_{ln}$	Left hub center position at Gait $i+1$
$c_{r0} \dots c_{ri} \dots c_{rn}$	Right hub center position at Gait $i+1$
$p_{0l} \dots p_{il} \dots p_{nl}$	Left foot position at Gait $i+1$
$p_{0r} \dots p_{ir} \dots p_{nr}$	Right foot position at Gait $i+1$

\* $i=0, 1, 2, \dots n$

#### 3.1.1 Useful Gait Parameterizations:

Useful parameters for describing gait pattern transition exist in these trajectories that each spoke follows. These parameters provide a form of semantic information about a gait, indicating the gait pattern, when certain spoke undergo stance,

as well as whether or not the gait will be valid to produce the expected locomotion.

### 1. Constraints:

First of all, physical and geometrical constraints are our principal concern. For the sake of simplicity, we only focus on right turning in this paper, that is, in the condition of  $l_{l0} \geq l_{r0}$ . The physical geometry of *IMPASS* gives us the following constraints:

$$l_{\min} = d_{\min} = 3.5\text{in}; l_{\max} = d_{\max} = 19\text{in} \quad (1)$$

$$\Delta l_{\min} = 0; \Delta l_{\max} = 15.5\text{in}$$

Combining the definition in Table 1, and the geometrical characters illustrated in Fig. 3, the following relationships could be derived:

$$\Delta l_0 = l_{l0} - l_{r0}; L_{d0} = \sqrt{L^2 + \Delta l_0^2} \quad (2)$$

The medial curvature ranges that 1-1P gait could reach is given in eq.(3). The derivation is presented in detail in eq. (15).

$$0 < \frac{1}{r_m} < \frac{1}{6.08 \text{ in}} \quad (3)$$

### 2. Two degrees of freedom:

1-1P has two degrees of freedom, as indicated in previous work [5], named as  $d_0$  and  $\theta_0$  for the Gait 1. For legibility 1-1P parallel topology has been transformed to the equivalent serial manipulator with two degrees of freedom (in Fig.4), which is also presented in [5]. The first degree of freedom  $d_0$  is caused by changing the lengths of the two spoke links simultaneously, which is a translational motion parallel to the spokes. The other degree of freedom  $\theta_0$  is the rotation of the pivoting line on the ground.

From the above definition, the first degree of freedom  $d_0$  is calculated by:

$$d_0 = \frac{l_{l0} + l_{r0}}{2} \quad (4)$$

Here, the other degree of freedom  $\theta_0$  corresponds to the dihedral angle between the plane where the first pair of spokes locate and the ground. Based on the geometry in Fig.5, the other degree of freedom  $\theta_0$  can be expressed by:

$$\sin \theta_0 = \frac{c_{l0} N_1}{c_{l0} N_0} \quad (5)$$

Where,  $N_1$  is the projected point of the left hub center  $c_{l0}$  on the ground, and at the same time, we make sure that  $N_1 N_2 \perp p_{0l} p_{1l}; N_0 N_1 \perp o_1 p_{0l}$ .

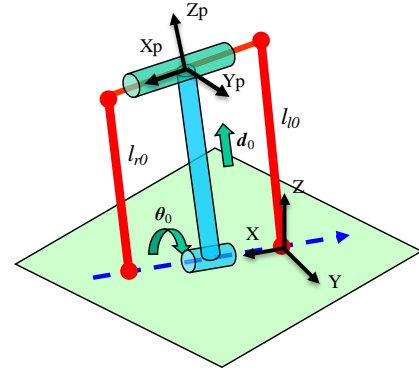


**Figure 4.** Degrees of Freedom of 1-1P Gait Pattern.

After some algebraic calculation by applying the trigonometric function, the constraint of the degree of freedom  $\theta_0$  is demonstrated in eq. (6). The detail steps of derivation are not presented here for concision.

$$\theta_{0\min} = \text{ArcSin} \left[ \frac{l_{\min} \text{Sin}(\frac{\pi}{3})}{\sqrt{l_{\min}^2 + l_{\max}^2 - l_{\min} l_{\max}}} \right] = 10.0^\circ \quad (6)$$

$$\theta_{0\max} = \text{ArcCot} \left[ L * \frac{\frac{2 * d_{0\min}}{d_{1\max}(\theta_0)} - 1}{\sqrt{3} \sqrt{L^2}} \right] = 110.0^\circ$$

Here, we'd like to notice that one degree of freedom of the next 1-1 P gait pattern  $d_1$  has very subtle relationship with  $d_0$  and  $\theta_0$ :

$$d_1 = \frac{2L}{L + \sqrt{3} \sqrt{L^2 + \Delta l_0^2} * \text{Cot}(\theta_0)} * d_0 \quad (7)$$

Where, three perpendicular line theorem in space analytic geometry is applied in the derivation of this expression and the following three useful angles' expression. The calculations are all overlapped in this paper. Please contact the corresponding author, for more details.

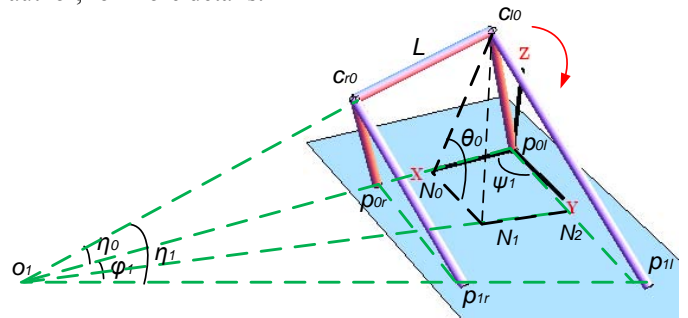


**Figure 5.** 1-1P Stance Geometry from Gait 1 to Gait 2.

### 3. Three Useful Angles:

Again, 1-1P performs the circular turning motion, therefore, three very vital angles  $\eta$ ,  $\psi$  and  $\varphi$  (see Fig. 5) are defined in

order to depict the gait function with clarity. The expressions and margins of each angle are demonstrated as follows:

The **Rolling Angle  $\eta_i$** : is the angle of the axle departure from the X Axis in their respective reference coordinate system at each Gait  $i$ . It is only the function of the effective spoke length difference of the parallel ground contact left and right spokes:

Gait 1:

$$\eta_0 = \text{ArcTan}\left(\frac{\Delta l_0}{L}\right); 0^\circ \leq \eta_0 \leq 44.1^\circ$$

Gait 2:

$$\eta_1(\theta_0) = \text{ArcTan}\left(\frac{\Delta l_1(\theta_0)}{L}\right); 0^\circ \leq \eta_1 \leq 86.4^\circ$$

Where,

$$\Delta l_1(\theta_0) = \frac{2L\Delta l_0}{L + \sqrt{3}L_{d0}\text{Cot}(\theta_0)} \quad (8)$$

The **Heading Angle  $\psi_i$**  defines the departure angle of the walking direction from the X Axis in their respective reference coordinate of Gait  $i$ , where the walking direction is corresponding to the ground contact left/right foot direction from gait to Gait  $i$  to Gait  $i+1$ .

$$\psi_1(\theta_0) = \text{ArcTan}\left(\frac{L}{\Delta l_0 * \text{Cos}(\theta_0)}\right)$$

$$\psi_{1max} = \text{ArcTan}\left(\frac{L}{\Delta l_{0max} * \text{Cos}(\theta_{0max})}\right) = 108.4^\circ \quad (9)$$

$$\psi_{1min} = \text{ArcTan}\left(\frac{L}{\Delta l_{0max} * \text{Cos}(\theta_{0min})}\right) = 46.3^\circ$$

The **Turning Angle  $\phi_i$**  is the rotating angle of the left or right feet about the turning center  $O_i$  from Gait  $i$  to Gait  $i+1$ .

$$\phi_1(\theta_0) = \text{Cos}^{-1}\left(\frac{L_{d0} + \sqrt{3}L\text{Cot}(\theta_0)}{\sqrt{4\Delta l_0^2 + (L + \sqrt{3}L_{d0}\text{Cot}(\theta_0))^2}}\right) \quad (10)$$

### 3.1.2 1-1P Forward and Inverse Kinematic Solutions:

The coordinate frames using DH convention is parameterized in order to obtain the forward transformation matrix and then deduce the following closed form forward and inverse kinematic solutions of 1-1P Gait Pattern. For the sake of concision, only the analytical solutions are presented here.

Analytical solution of forward kinematics:

$$\begin{aligned} q_x &= \frac{L_{d0}}{2} + d_0 \text{Sin}(\eta_0) \\ q_y &= -d_0 \text{Cos}(\eta_0) \text{Cos}(\theta_0) \\ q_z &= d_0 \text{Cos}(\eta_0) \text{Sin}(\theta_0) \end{aligned} \quad (11)$$

Analytical solution of inverse kinematics:

$$\begin{aligned} d_0 &= \frac{q_x - L_{d0}/2}{\text{Sin}(\eta_0)} \\ \theta_0 &= \text{ArcSin}\left[\frac{-q_y \text{Sin}(\eta_0)}{\text{Cos}(\eta_0)(q_x - L_{d0}/2)}\right] \\ &\text{or} \\ \theta_0 &= \text{ArcCos}\left[\frac{q_z \text{Sin}(\eta_0)}{\text{Cos}(\eta_0)(q_x - L_{d0}/2)}\right] \end{aligned} \quad (12)$$

The position coordinates of hub centers  $c_{l0}$ ,  $c_{r0}$  expressed in the global coordinates are given by:

$$\begin{aligned} c_{l0} &\left(\frac{L_{d0}}{2} + d_0 \text{S}(\eta_0) - \frac{L}{2} \text{C}(\eta_0), \right. \\ &\quad \left. \left(d_0 \text{C}(\eta_0) + \frac{L}{2} \text{S}(\eta_0)\right) \text{C}(\theta_0), \left(d_0 \text{C}(\eta_0) + \frac{L}{2} \text{S}(\eta_0)\right) \text{S}(\theta_0)\right) \\ c_{r0} &\left(\frac{L_{d0}}{2} + d_0 \text{S}(\eta_0) + \frac{L}{2} \text{C}(\eta_0), \right. \\ &\quad \left. \left(d_0 \text{C}(\eta_0) - \frac{L}{2} \text{S}(\eta_0)\right) \text{C}(\theta_0), \left(d_0 \text{C}(\eta_0) - \frac{L}{2} \text{S}(\eta_0)\right) \text{S}(\theta_0)\right) \end{aligned}$$

Here  $S$  denotes  $\text{Sin}$  and  $C$  denotes  $\text{Cos}$  in above expressions.

### 3.1.3 Feasible Footprints of Gait 2 for 1-1P:

The potential area of the next gait footprints is worthwhile to study for the future path planning. First of all, the coordinate transformation matrix is used to convert the reference coordinates from the stance of the current gait to the stance of the next gait, both denoted in the global coordinate. For example, in Fig.6,  $H_0^1$  is the transformation matrix from the reference coordinate of Gait 1  $XYZ$  to the reference coordinate of Gait 2  $X_1Y_1Z_1$ :

$$H_0^1 = \begin{bmatrix} \text{Cos}(\phi_1) & \text{Sin}(\phi_1) & 0 & \Delta l_1 \text{Cos}(\psi_1) \\ -\text{Sin}(\phi_1) & \text{Cos}(\phi_1) & 0 & \Delta l_1 \text{Sin}(\psi_1) \\ 0 & 0 & 1 & 0 \\ 0 & 0 & 0 & 1 \end{bmatrix}$$

Here

$$\begin{aligned} \Delta l_1 &= \Delta l_1(d_0, \theta_0) \\ &= \frac{d_0 + \Delta l_0/2}{\sqrt{3}L_{d0}\text{Cos}(\theta_0) + L\text{Sin}(\theta_0)} \sqrt{3(L^2 + \Delta l_0^2 \text{Cos}^2(\theta_0))} \end{aligned} \quad (13)$$

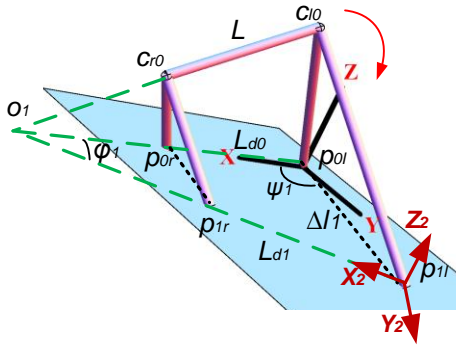


**Figure 6.** Global Coordinate Transformation from Gait 1 to Gait 2.

Then the next feet location  $p_{1l}, p_{1r}$  in the global coordinates is identified by:

$$p_{1l} (\Delta l_1 C(\psi_1), \quad \Delta l_1 S(\psi_1), \quad 0)$$

$$p_{1r} (\Delta l_1 C(\psi_1) + L_{d1} C(\varphi_1), \quad \Delta l_1 S(\psi_1) - L_{d1} S(\varphi_1), \quad 0)$$

$$\text{where, } L_{d1} = L_{d1}(\theta_0) = \sqrt{L^2 + \Delta l_1(\theta_0)^2}$$

Note:  $S$  denotes  $Sin$  and  $C$  denotes  $Cos$  in above expressions.

Fig.7 shows the potential feasible next pair footprints of Gait 2. The blue straight line indicates the possible position range when  $d_0$  changes whereas  $\theta_0$  is fixed. The red curve is corresponding to the potential range when  $\theta_0$  changes whereas  $d_0$  is fixed. The arrow points the increasing direction of  $d_0$  and  $\theta_0$  and respectively.

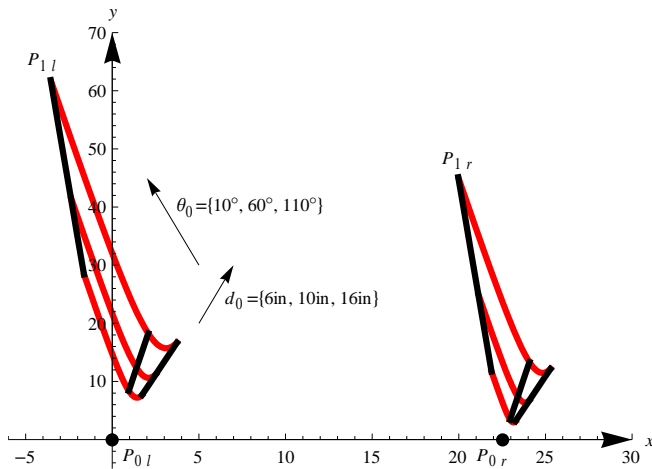


**Figure 7.** Feasible Footprints of Gait 2 for 1-1 P.

### 3.1.4 Trajectory Generation of 1-1P Gait:

Path planning from the initial point to the target point is basically composed of circle segment and straight line segment. In order to follow a circle path, the following assumption will be made:

$$\Delta l_0 = \Delta l_1 = \dots = \Delta l_i = \dots = \Delta l_n$$

That is:

$$\tan^{-1} \sqrt{3(1 + (\frac{\Delta l_0}{L})^2)} \leq \theta_0 \leq \frac{\pi}{3}$$

Then the turning angle turns out to be:

$$\varphi_i(\Delta l_0) = \cos^{-1} \left( \frac{L_{di} + L}{\sqrt{4\Delta l_i^2 + (L + L_{di})^2}} \right) \quad (14)$$

Where,

$$L_{di} = \sqrt{L^2 + \Delta l_i^2}; 0^\circ \leq \varphi_i \leq 32.34^\circ$$

The minimum steps to finish a circle become:

$$N_{min} = 12$$

The radius of the outside, inside and medial concentric circle is given by:

$$r_{oi} = \left( \pm \frac{1}{2} + \frac{d_i}{L_i} \right) \sqrt{L^2 + \Delta l_i^2}; r_m = \frac{d_i}{L_i} \sqrt{L^2 + \Delta l_i^2} \quad (15)$$

$$33.0 \text{ in} \leq r_o \leq \infty; 6.1 \text{ in} \leq r_i \leq \infty; 19.5 \text{ in} \leq r_m \leq \infty$$

The following trajectory gives us the footprints of *IMPASS* when it follows the circle with the values of

$$\varphi = 30^\circ, r_o = 35.38 \text{ in}, r_i = 9.38 \text{ in}, r_m = 26.0 \text{ in} \quad (16)$$

$$\text{when } d_0 = 11.93 \text{ in}, \Delta l_0 = 13.86 \text{ in}$$

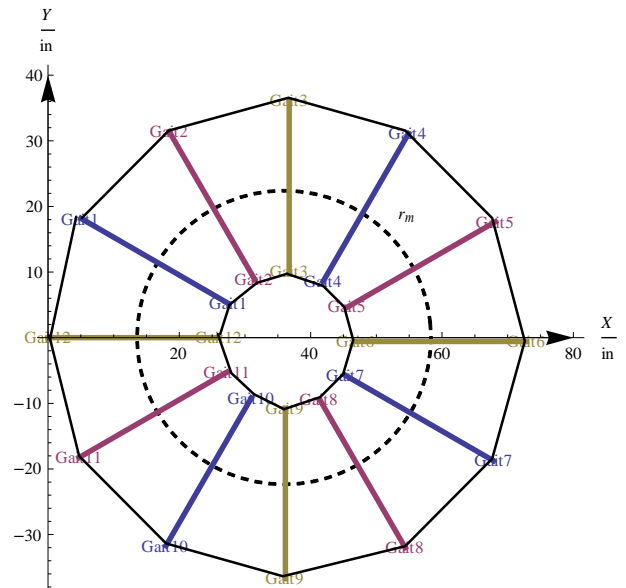


**Figure 8.** Top View of Circular Trajectory for 1-1P Gait.



walking area of the next gait, which is important for trajectory transition from circular turn to straight line walking.

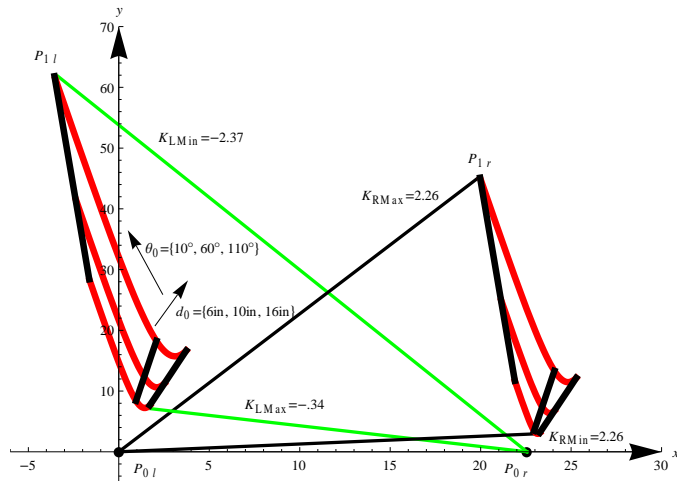


**Figure 11.** Feasible Footprints and Straight Line Walking Area of 1-1P to 1-1S Gait Transition

#### 4 EXPERIMENT AND DISCUSSION

Open loop stable control strategies have been applied for the gait transitions. By control strategy we mean the way a movement system structures itself to approach a task. An open loop stable control strategy does not use active reaction to respond to perturbations. It uses the geometry of the mechanical device, the kinematics and dynamics of motion, and the properties of materials to stabilize the task execution. It is distinguished from closed loop control strategies by the absence of sensory input to the computing of actuator commands for error compensation.

In this section, several typical gait pattern transition tasks will be discussed to illuminate issues of the applications of open loop strategies on gait transitions.

##### 4.1 1-1 P Gait Turning Motion:

1-1P gait pattern has been adopted to perform circular turning with constant curvature. This gait pattern sets a smaller curvature for the outside hub and a larger curvature for the inside hub, as shown in Fig. 12 (a). Testing was done to correlate the predicted inner turning radius of 18 inches with the actual turning curvature, displayed as the white circle in Fig. 12(a). The prototype performed maneuver with an inner turning radius actually ranging from 18 inches to 20 inches. The deviation from the rigid kinematic model to the physical prototype is the result of several reasons, including the offset of the spokes in the hub, the compliance of the spokes, as well as the physical size of the feet. Also, the feet do not make a perfectly discrete contact point with the ground while taking a step, but rather roll over approximately an inch, introducing a slight variation from the kinematic model.

Another observation from the circular turning motion testing was an unexpected twisting of the spokes during a turn, as

shown in Fig. 12 (b). This twist occurs as IMPASS walks over the foot at an angle, allowing the flat sides of the feet to hold the ground. A possible solution to this twist is the change from a flat-sided foot to a ball foot, eliminating the flat edge.

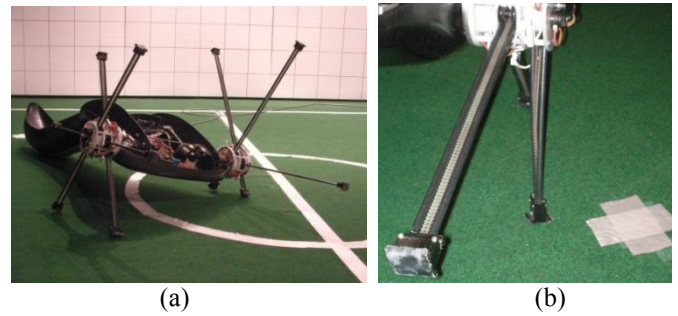


**Figure 12.** Snapshot of (a) Circular Turning Motion using 1-1P Gait Pattern (b) Spoke Twisting

##### 4.2 1-1 S Turning Gait Transition:

The turning gait transition is used to transform between circular line turning and straight line waling, or between different curvature circular lines turning. The snapshot of 1-1 Skew gait transition pattern is illustrated in Fig. 13. In this test, the prototype performed as predicted by the kinematic model, and did not show any sign of instability. Since 1-1 Skew pattern allows IMPASS to change the roll orientation of the body with slight flex in the spokes during this transition motion, the prototype of IMPASS remains stable and controllable over this range of motion.



**Figure 13.** Snapshot of 1-1S Gait Transition Pattern

#### 5 CONCLUSIONS AND FUTURE RESEARCH

Through a greater understanding of gait patterns, we have shown how gait pattern transitions lead to new behaviors of IMPASS, such as steering. Switching between gaits instantaneously or switching between spokes progressively, results in motion patterns that continue locomotion, while keeping the robot's configuration valid.

Future directions for this research branch out in a variety of ways. Our newfound understanding of gait patterns is allowing

us to consider a continuum of gaits, rather than isolated gaits. Using this continuous representation, we intend to apply control by evolving a gait over time, performing local feedback by applying touch or/and vision sensors. We are also interested in techniques of trajectory and path planning, to encode gaits and gait transitions in a continuous framework.

## 6 ACKNOWLEDGMENTS

The authors would like to thank Blake Jeans, Shawn Kimmel and the senior design team members under his lead for developing excellent robotic platforms for research. This work was supported by the National Science Foundation under Grant No. 0535012.

## 7 REFERENCES

- [1] Laney, D. and Hong, D.W., "Kinematic Analysis of a Novel Rimless Wheel with Independently Actuated Spokes", 29<sup>th</sup> ASME Mechanisms and Robotics Conference, Long Beach, California, September 24-28, 2005.
- [2] Hong, D.W. and Laney, D., "Preliminary Design and Kinematic Analysis of a Mobility Platform with Two Actuated Spoke Wheels", US-Korea Conference on Science, Technology and Entrepreneurship (UKC 2006), Mechanical Engineering & Robotics Symposium, Teaneck, New Jersey, August 10-13, 2006.
- [3] Laney, D. and Hong, D.W., "Three-Dimensional Kinematic Analysis of the Actuated Spoke Wheel Robot". 30<sup>th</sup> ASME Mechanisms and Robotics Conference, Philadelphia, Pennsylvania, September 10-13, 2006.
- [4] P. Ren, J. Jeans, D. Hong, "Kinematics Analysis and Experimental Verification on the Steering Characteristics of a Two Actuated Spoke Wheel Robot with a Tail," 33<sup>rd</sup> ASME Mechanisms and Robotics Conference, August 30-September 2, 2009, San Diego, California, USA
- [5] Y. Wang, P. Ren, D. Hong, "Mobility and Geometrical Analysis of a Two Actuated Spoke Wheel Robot Modeled as a Mechanism with Variable Topology," 32<sup>nd</sup> ASME Mechanisms and Robotics Conference, August 3-6, 2008, Brooklyn, New York, USA.
- [6] P. Ren, Y. Wang, D. Hong, "Three-dimensional Kinematic Analysis of a Two Actuated Spoke Wheel Robot Based on its Equivalency to A Serial Manipulator," 32<sup>nd</sup> ASME Mechanisms and Robotics Conference, August 3-6, 2008, Brooklyn, New York, USA.
- [7] R. Altendorfer, N. Moore, H. Komsuoglu, M. Buehler, H.B. Borown, D. McMordie, U. Saranli, R. Full, and D. Koditschek. "Rhex: A biologically inspired hexapod runner," *Autonomous Robots*, vol. 11, p.207, 2001.
- [8] J.D. Weingarten, G.A.D. Lopes, M. Buehler, R. E. Groff, and D.E. Koditschek, "Automated gait adaptation for legged robots," *IEEE Int. Conf. on Robotics and Automation (ICRA)*, vol. 3, 2004, pp. 2153-2158.
- [9] S.Schaal and C.G. Atkeson, "Open Loop Stable Control Strategies for Robot Juggling," *IEEE International Conference on Robotics and Automation (ICRA)*, vol. 3, GA, Atlanta, 1993, pp. 913-918.
- [10] R.B. McGhee, and G.I. Iswandhi, "Adaptive Locomotion of a Multilegged Robot over Rough Terrain," *IEEE Trans. Syst., Man, Cybern. SMC-9(4)* 176-182, 1979.
- [11] S.M. Song and K.J. Waldron, "An Analytical Approach for Gait Study and Its Applications on Wave Gait," *The International Journal of Robotics Research*, 6(2), summer, 1987.
- [12] S. Hamdan, J.G. Fontaine, and M. Picard, "Theoretical Approach to Gait Transition," *Proceedings of the 8<sup>th</sup> CISM-IFTOMM Symposium on Theory and Practice of Robots and Manipulators*, Cracow, Poland, July 2-5, 1990, pp. 366-375.
- [13] C.D. Zhang and S.M. Song, "Turning Gaits of a Quadrupedal Walking Machine," *IEEE International Conference on Robotics and Automation (ICRA)*, Sacramento, CA, USA, April 9-11, 1991, vol.3, pp. 2106-2112.
- [14] K. Tsujita, T. Kobayashi, T. Inoura and T. Masuda, "A Study on Adaptive Gait Transition of Quadruped Locomotion," *SICE Annual Conference*, Tokyo, Japan, August 20-22, 2008, pp. 2489-2494.
- [15] G.C. Haynes and A.A. Rizzi, "Gait and Gait Transitions for Legged Robots," *IEEE International Conference on Robotics and Automation (ICRA)*, Orlando, Florida, USA, May, 2006, pp. 1117-1122.